Comparative Study of Mode-Matching Formulations for Microstrip Discontinuity Problems

TAK SUM CHU, TATSUO ITOH, FELLOW, IEEE, AND YI-CHI SHIH, MEMBER, IEEE

Abstract—**Several matrix formulations for the microstrip step-discontinuity problem are compared. Although they are theoretically identical, one of them has an advantage in numerical labor, relative, and absolute convergence. Results of this method are checked with other published data and with those independently obtained by the modified residue calculus technique.**

I. Introduction

A STEP DISCONTINUITY is frequently encountered in microstrip line circuits and, hence, its analysis is important for circuit design. There are several approaches available. When the microstrip is enclosed in a waveguide-like case, it is possible to calculate the fundamental and higher order modes in both sides of the step and to impose the continuity conditions of the tangential field in the cross section of the shield case at the step location. This process leads to a system of mode-matching equations. When an open microstrip line circuit is dealt with, the higher order modes can become radiation modes which must be included in the mode-matching procedure.

In many applications, the so-called waveguide model has been found useful for calculation of the scattering at the microstrip discontinuity [1]–[3]. In this paper, we assume that the waveguide model is an acceptable technique for the calculation of the step-continuity problem. In addition, radiation and surface waves are not considered. The motivation for the present work is somewhat different from those published. Although a number of numerical data are presented in the literature [1]–[3], details of the numerical process are not clear. The objective of the present paper is not to duplicate the numerical data already available, but to place some foundation on how these data should be calculated. We present several alternative formulations. Although these formulations are theoretically identical, it is pointed out that the numerical labor and accuracy depend on the choice of formulation and some are better than others.

Manuscript received February 4, 1985; revised May 14, 1985. This work was supported in part by the U.S. Army Research Office under Contract DAAG 29-84-k-0076.

T. S. Chu and T. Itoh are with the Department of Electrical and Computer Engineering, University of Texas, Austin, TX 78712.

Y-C. Shih is with Hughes Aircraft Company, Microwave Products Division, Torrance, CA 90509.

Fig. 1. The waveguide model of the open microstrip line.

The best formulation can be decided based on the matrix size, relative and absolute convergence, and other numerical considerations. It turns out that the best formulation is the one we often choose without clear reasoning. The data for a microstrip step discontinuity are compared with available data. They are also compared with the modified residue calculus technique, which serves as an independent check of the numerical accuracy.

Before starting the formulation, let us briefly review the waveguide model. In this technique, the uniform microstrip line of width w_0 on the substrate of height h and relative dielectric constant ϵ_r is replaced with an equivalent parallel-plate waveguide with magnetic side walls (Fig. 1). The substrate height is kept identical. However, the effective width w_{eff} and the effective dielectric constant ϵ_{eff} are used to define the effective waveguide in such a way that the effect of the fringing field of the microstrip is taken into account. Specifically, these effective values are related to the propagation constant β and the characteristic impedance Z_0 via

$$\epsilon_{\text{eff}} = (\beta/k_0)^2$$

$$Z_0 = \left(120\pi/\sqrt{\epsilon_{\text{eff}}}\right)(h/w_{\text{eff}}). \tag{1}$$

Note that β and Z_0 can be found from a standard analysis such as the spectral-domain method, from curve fitting, or an empirical formula, once the structural parameters of the microstrip line are given.

For the analysis of the step discontinuity, both sides of the step are replaced with their respective equivalent waveguides. Note that the heights of these two waveguides are identical. Hence, the problem remains a two-dimensional one as the field is uniform in the y- (vertical) direction. Also, note that the dominant mode in the equivalent waveguide is TEM. In the following sections, all structural parameters used, except h, are presumed to be the "effective" ones, unless otherwise stated.

0018-9480/85/1000-1018$01.00 ©1985 IEEE

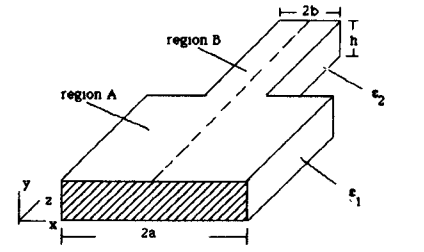

(a)

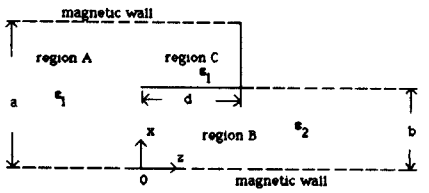

(b)

Fig. 2. (a) Waveguide model for symmetric microstrip step discontinuity. (b) Auxiliary geometry for the waveguide problem.

II. Formulation

The problem under study is the waveguide model for the microstrip step discontinuity shown in Fig. 2(a). The structure is assumed to be symmetrical, and the parallel-plate waveguide is idealized with magnetic side walls. For convenience of analysis, an auxiliary structure is introduced in Fig. 2(b). Only one half of the original structure is considered because of symmetry, and the transversal magnetic wall at the discontinuity is recessed to create a new region C. The original structure is recovered by letting $d = 0$.

The mode-matching procedure begins by expanding the tangential electric and magnetic fields at the junction in terms of the normal modes on both sides of the junction. For TE_{n0} $(n = 0,1,\cdots)$ excitation, we write down the E_y continuity equation

$$\sum_{n=0}^{M-1}(A_n^+ + A_n^-)\phi_{an} = \begin{cases} \sum_{n=0}^{K-1}(B_n^+ + B_n^-)\phi_{bn}, & 0 \le x \le 0 \\ \sum_{n=0}^{L-1} C_n\phi_{cn}(1+\rho_n), & b \le x \le a \end{cases} \tag{2a}$$

and a corresponding one for H_x

$$\sum_{n=0}^{M-1}(A_n^+ - A_n^-)Y_{an}\phi_{an} = \sum_{n=0}^{K-1}(B_n^+ - B_n^-)Y_{bn}\phi_{bn}, \quad 0 \le x \le b$$

$$= \sum_{n=0}^{L-1} C_n Y_{cn}\phi_{cn}(1-\rho_n), \quad b \le x \le a \tag{2b}$$

where

$$\phi_{an} = \sqrt{(\epsilon_{n0}/a)}\cos(k_{an}x), \qquad k_{an} = (n\pi/a)$$
$$\phi_{bn} = \sqrt{(\epsilon_{n0}/b)}\cos(k_{bn}x), \qquad k_{bn} = (n\pi/b)$$
$$\phi_{cn} = \sqrt{(\epsilon_{n0}/c)}\cos(k_{cn}(a-x)), \qquad k_{cn} = (n\pi/c)$$
$$\epsilon_{n0} = \begin{cases} 1, & n = 0 \\ 2, & n \ne 0 \end{cases}$$

and

$$Y_{an} = \sqrt{\left(\epsilon_1 k_0^2 - (n\pi/a)^2\right)} = \beta_n$$
$$Y_{bn} = \sqrt{\left(\epsilon_2 k_0^2 - (n\pi/b)^2\right)} = \gamma_n$$
$$Y_{cn} = \sqrt{\left(\epsilon_1 k_0^2 - (n\pi/c)^2\right)} = \bar{\beta}_n$$
$$\rho_n = \exp(-2j\bar{\beta}_n d).$$

In (2), ϕ_{an}, ϕ_{bn}, and ϕ_{cn} are normal modes in Regions A, B, and C, with propagation constants β_n, γ_n, and $\bar{\beta}_n$, respectively. A_n^+ and B_n^- are the given incident field coefficients from Regions A and B (usually only one A_n^+ or B_n^- is considered at a time), while A_n^-, B_n^+, and C_n are the unknown excited field coefficients in regions A, B, and C, respectively. ρ_n is the reflection from the magnetic wall in Region C.

From modal orthogonality, we obtain the linear simultaneous equations for the unknown modal coefficients

$$A_m^+ + A_m^- = \sum_{n=0}^{K-1} H_{mn}(B_n^+ + B_n^-) + \sum_{n=0}^{L-1} \bar{H}_{mn}C_n(1+\rho_n)$$

$$Y_{am}(A_m^+ - A_m^-) = \sum_{n=0}^{K-1} H_{mn}Y_{bn}(B_n^+ - B_n^-) + \sum_{n=0}^{L-1} H_{mn}Y_{cn}C_n(1-\rho_n),$$
$$m = 0,1,2,\cdots,M-1 \tag{3a}$$

$$\sum_{n=0}^{M-1} H_{nm}(A_n^+ + A_n^-) = B_m^+ + B_m^-$$

$$\sum_{n=0}^{M-1} H_{nm}Y_{an}(A_n^+ - A_n^-) = Y_{bm}(B_m^+ - B_m^-),$$
$$m = 0,1,2,\cdots,K-1 \tag{3b}$$

$$\sum_{n=0}^{M-1} \bar{H}_{nm}(A_n^+ + A_n^-) = C_m(1+\rho_m)$$

$$\sum_{n=0}^{M-1} \bar{H}_{nm}Y_{an}(A_n^+ - A_n^-) = C_m Y_{cm}(1-\rho_m),$$
$$m = 0,1,2,\cdots,L-1 \tag{3c}$$

where

$$H_{mn} = \int_0^b \phi_{am}\phi_{bn}\,dx = \left(\frac{\epsilon_{m0}\epsilon_{n0}}{ab}\right)^{1/2}\left(\frac{1}{2}\right)\left(\frac{2k_{am}(-1)^n\sin(k_{am}b)}{k_{am}^2 - k_{bn}^2}\right)$$

$$\bar{H}_{mn} = \int_b^a \phi_{am}\phi_{cn}\,dx = \left(\frac{\epsilon_{m0}\epsilon_{n0}}{ac}\right)^{1/2}\left(\frac{1}{2}\right)\left(\frac{2k_{am}(-1)^{n+1}\sin(k_{am}b)}{k_{am}^2 - k_{cn}^2}\right).$$

To condense the above equations, we define the following matrices:

$$Y_i = \begin{bmatrix} Y_{i0} & 0 & \cdots & \\ & Y_{i1} & & \\ 0 & & Y_{i2} & \\ \vdots & & & \ddots \\ & & & Y_{in} \end{bmatrix},$$

$$i = a, b, c$$
$$n = M-1, K-1, L-1,$$

$$R = \begin{bmatrix} 1+\rho_0 & 0 & \cdots & \\ 0 & 1+\rho_1 & & \\ \vdots & & \ddots & \\ & & & 1+\rho_n \end{bmatrix}$$

$$R' = \begin{bmatrix} 1-\rho_0 & 0 & \cdots & \\ & 1-\rho_1 & & \\ 0 & & \ddots & \\ \vdots & & & 1-\rho_n \end{bmatrix}$$

$$n = L-1$$

$$Y_d = \left[\begin{array}{c|c} Y_b & 0 \\ \hline 0 & Y_c \end{array}\right] \quad \bar{R}' = \left[\begin{array}{c|c} I & 0 \\ \hline 0 & R' \end{array}\right] \quad \bar{R} = \left[\begin{array}{c|c} I & 0 \\ \hline 0 & R \end{array}\right]$$

$$G = [H \mid \bar{H}]$$

where I is the identity matrix, H is a matrix of size $M \times K$ with generic element H_{mn} as defined above, while $\bar{H}$ is a matrix of size $M \times L$ with generic element $\bar{H}_{mn}$.

Then, the mode-matching equations can be written in the following matrix form:

$$\underset{\sim}{a}^+ + \underset{\sim}{a}^- = G\bar{R}\underset{\sim}{d}^+ + G\underset{\sim}{d}^- \tag{4a}$$

$$Y_a(\underset{\sim}{a}^+ - \underset{\sim}{a}^-) = GY_d\bar{R}'\underset{\sim}{d}^+ - GY_d\underset{\sim}{d}^- \tag{4b}$$

$$G^T(\underset{\sim}{a}^+ + \underset{\sim}{a}^-) = \bar{R}\underset{\sim}{d}^+ + \underset{\sim}{d}^- \tag{4c}$$

$$G^TY_a(\underset{\sim}{a}^+ - \underset{\sim}{a}^-) = Y_d\bar{R}'\underset{\sim}{d}^+ - Y_d\underset{\sim}{d}^- \tag{4d}$$

where superscript T denotes transpose operation, and

$$\underset{\sim}{a}^+ = \begin{bmatrix} A_0^+ \\ A_1^+ \\ A_2^+ \\ \vdots \\ A_{M-1}^+ \end{bmatrix} \quad \underset{\sim}{d}^- = \begin{bmatrix} B_0^- \\ B_1^- \\ \vdots \\ B_{K-1}^- \\ \hline 0 \\ \vdots \\ 0 \end{bmatrix}$$

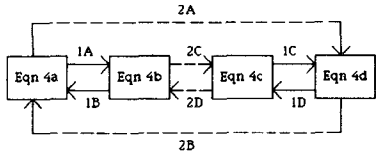

Fig. 3. Classification of formulations.

$$\underset{\sim}{d}^+ = \begin{bmatrix} B_0^+ \\ B_1^+ \\ \vdots \\ B_{K-1}^+ \\ \hline C_0 \\ C_1 \\ \vdots \\ C_{L-1} \end{bmatrix} \quad \underset{\sim}{a}^- = \begin{bmatrix} A_0^- \\ A_1^- \\ A_2^- \\ \vdots \\ A_{M-1}^- \end{bmatrix}$$

$\underset{\sim}{a}^+$ and $\underset{\sim}{d}^-$ are column vectors of the excitation terms and $\underset{\sim}{a}^-$ and $\underset{\sim}{d}^+$ are column vectors of the unknown modal coefficients. All matrices are of size $(M \times M)$; this requires that $K + L = M$.

When $M \to \infty$, we can prove that $G^{-1} \equiv G^T$. Therefore, (4a) and (4b) are equivalent to (4c) and (4d). Two independent vector equations are required to solve for two unknown vectors. Hence, for four pairs of equations ((4a) and (4b), (4b) and (4c), (4c) and (4d), and (4d) and (4a)), substituting one equation into the other in the same pair, we have eight ways to solve for $\underset{\sim}{a}^+$ and $\underset{\sim}{d}^-$. They are defined graphically in Fig. 3. The approaches indicated by a solid arrow are classified as the formulations of the first kind and those indicated by a dashed arrow are of the second kind. Although the eight ways of solution are theoretically equivalent, their numerical behaviors are somewhat different, especially when the magnetic wall is introduced at the upper half of the junction ($d = 0$, $\rho_n = 1$).

For general cases $d \neq 0$, all the formulations require a matrix inversion of size $(M \times M)$. For our limiting case of $d = 0$, special modifications must be made for some cases. Specifically, 1D and 2B need to invert a $(M + L) \times (M + L)$ matrix and 2C (Appendix A) needs to invert a smaller $(K \times K)$ matrix. Hence, 2C is most attractive to us because of its potential of numerical efficiency. In the next section, we will examine the various approaches in terms of the numerical stability and convergence.

III. Numerical Results

To study the numerical behavior of the various formulations, we have chosen the structural parameters as: $a = 100$, $b = 26.1$ (in mils), $\epsilon_1 = 2.2$, $\epsilon_2 = 2.1$. The dominant mode (TEM) reflection and transmission coefficients at the junction are calculated by varying the matrix size for different K/M ratios.

Since formulations 1D and 2B have an apparent disadvantage in numerical calculations, they are not considered here. After extensive studies, we have found that 1A, 1B, and 1C are numerically identical. Similarly, 2A and 2D are

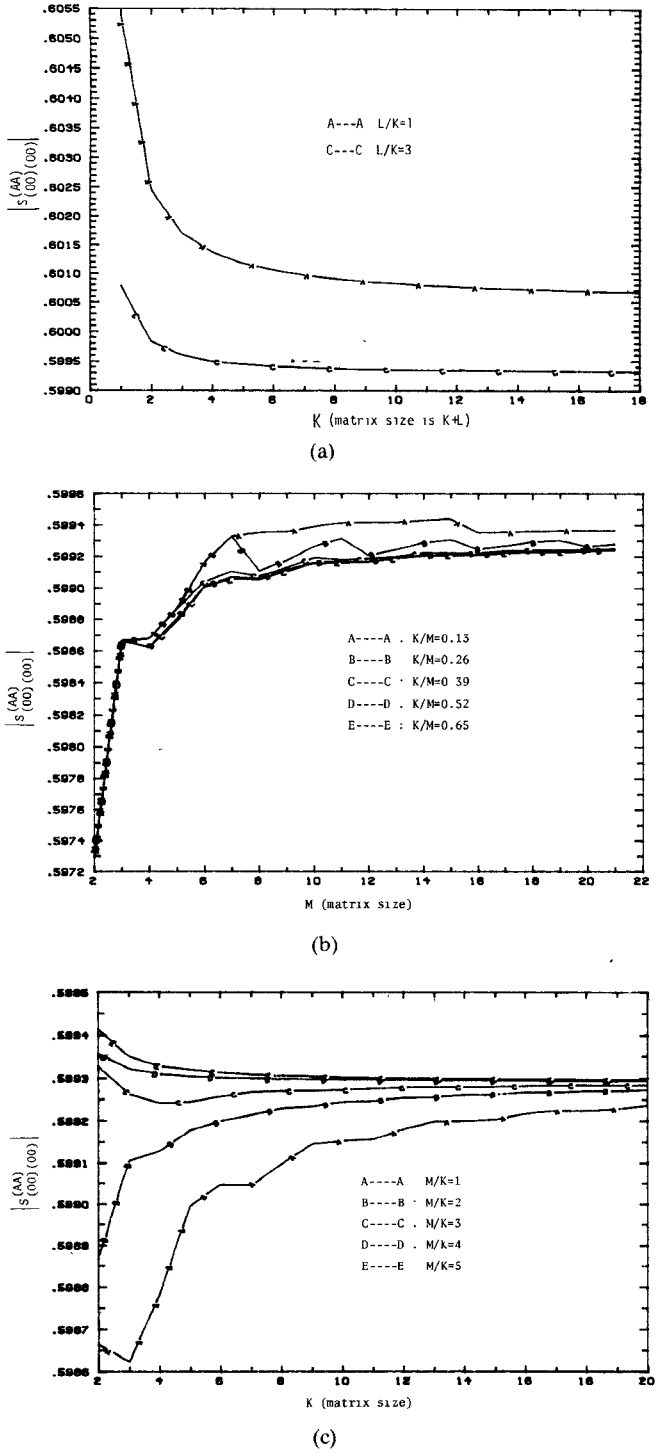

Fig. 4. Convergence study for various formulations: (a) formulation 1A; (b) formulation 2A; (c) formulation 2C.

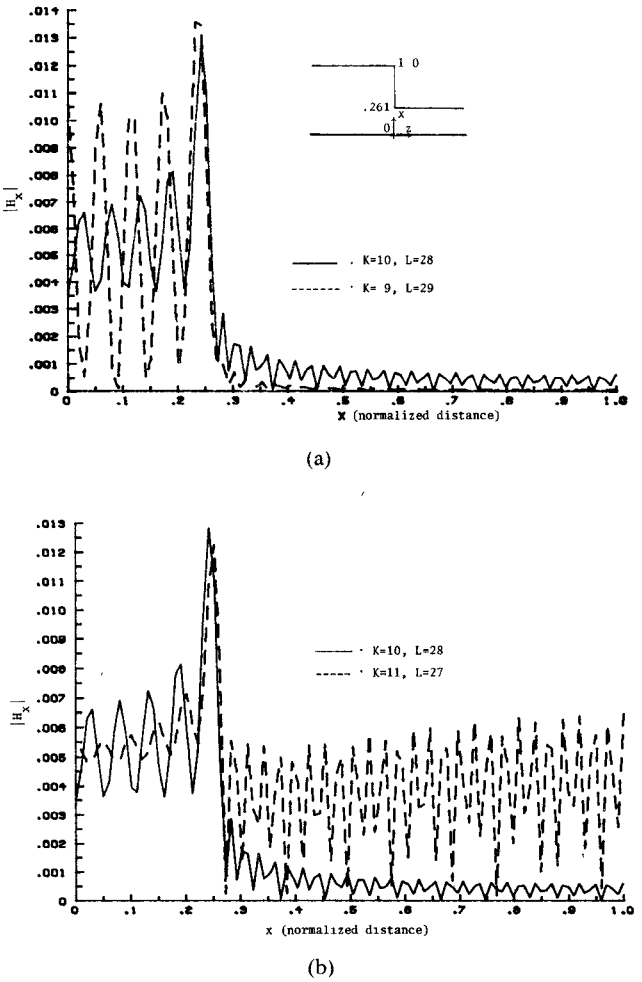

Fig. 5. Relative convergence problem of formulation 1A demonstrated by field plots.

numerically identical. Therefore, only three sets of data, corresponding to 1A, 2A, and 2C, are given.

In each formulation, the indices L, K, and M are involved. The numerical results are affected by the ratios among these indices. This is called the relative convergence phenomenon, and it has been thoroughly discussed in the literature [4], [5]. It is well known that the best approximation to the true solution is obtained for $L/K = c/b = 73.6/26.1$ or $M/K = a/b = 100/26.1$ (refer to as the right ratio). It is observed that 2A and 2C suffer very little from the relative convergence problem (Fig. 4(b) and (c)). The problem is more serious in 1A, as can be seen in Fig. 4(a). With a ratio of one, the dominant mode reflection coefficient converges to an incorrect value (curve A in Fig. 4(a)). Curve C is calculated using a ratio of three, which is close to the right ratio.

The relative convergence effect can be more clearly observed from the plot of H_x at the junction. The resultant field calculated by 1A is shown in Fig. 5. In Fig. 5(a), we plot the fields calculated using a ratio of $L/K = 28/10$ (very close to the right ratio) and a ratio of 29/9 (higher than the right ratio). In Fig. 5(b), we compare the field calculated using a ratio of 27/11 (lower than the right ratio) and a ratio of 28/10. It is interesting to note that, with a higher ratio, the calculated field behaves better on the magnetic wall discontinuity than on the aperture, while the opposite is true for field calculated using a lower ratio. This might seem reasonable because, for a higher ratio, we use more modes on the magnetic wall than on the aperture and vice versa for a lower ratio. Fig. 6 shows the resultant fields calculated by 2C. Different ratios have no noticeable effect. The fields calculated by 2A behave similar to those calculated by 2C.

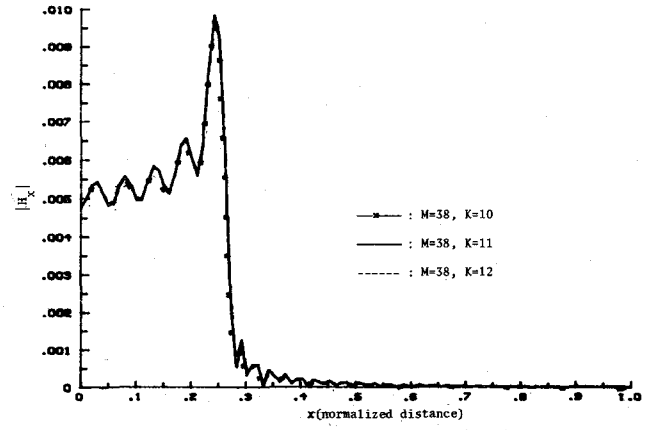

Fig. 6. Plot of fields calculated using formulation 2C with different M/K ratios.

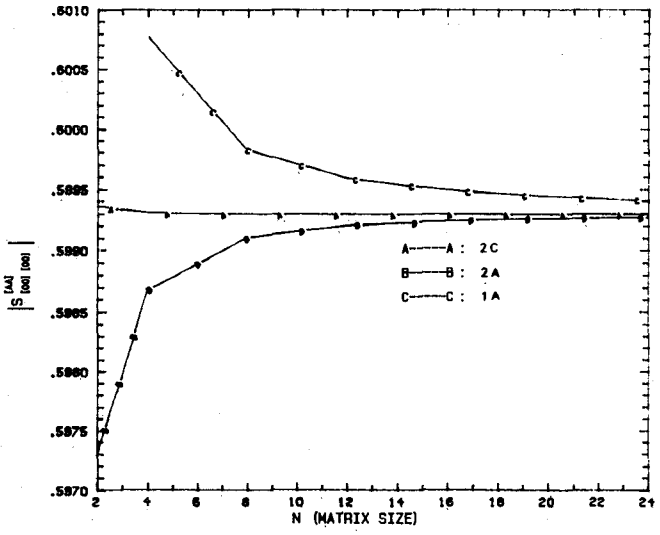

Fig. 7. Comparison of numerical efficiency.

A comparative study on the numerical efficiency for different approaches has also been done. In this case, $M/K = 4$, which is close to a/b, is chosen. The results of the dominant mode reflection coefficient $S[00][00]$ are evaluated as a function of the matrix size required and shown in Fig. 7. In addition, a comparison of how well the fields of the two sides match at the junction is done between formulations 2A and 2C. In both calculations, M is set to 40, K to 10. The result is shown in Fig. 8. The fields calculated by 2C match as well as, if not better than, those calculated by 2A. Keep in mind that we have to invert a matrix of size 40 in 2A, compared to a matrix of size 10 in 2C. It is now obvious that 2C has definite advantages over other approaches. This formulation is to be used for further studies.

Let us refer back to (2) at this point. In many attempts, E_y in the region $b < x < a$ is not used as $H_x = 0$ there. This is identical to 2C and, hence, is our preferred choice.

To check the validity of our calculations, we have calculated the frequency response of a microstrip step discontinuity using the same parameters given by Kompa [2]. The results of the dominant mode reflection and transmission coefficients $S[00][00]$ and $S[00][00]$ are shown in Fig. 9. They are in good agreement with Kompa's results. The small discrepancy is due to the different formulas used for obtaining the effective width and effective dielectric constant of the waveguide model. Furthermore, we have checked the results with those independently obtained by the modified residue calculus technique [6]. The results of $S[00][00]$ are shown in Table I and Fig. 10 for comparison. The calculations are performed using Kompa's parameters.

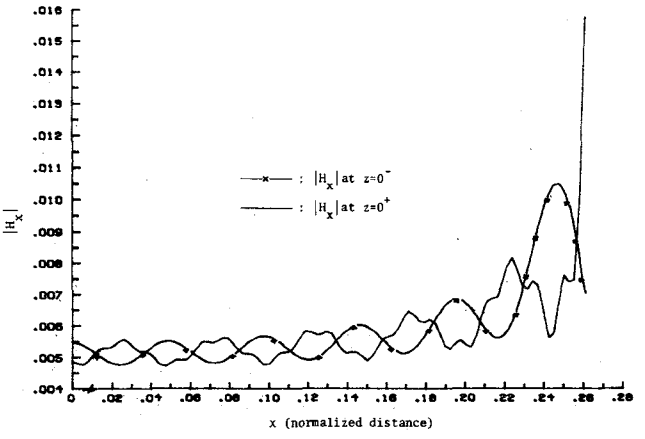

(a)

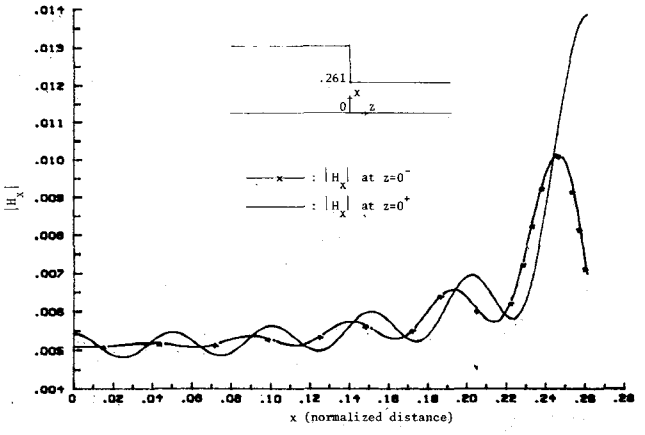

(b)

Fig. 8. Comparison of field plot between formulation 2A and 2C. (a) 2A, (b) 2C.

IV. Conclusion

The mode-matching method has been applied to analyze the microstrip step-discontinuity problem based on the waveguide model. A comparison has been made among the various mode-matching solutions based on the matrix size and relative and absolute convergence. Although they are theoretically identical, one of them proves to be most suitable for numerical calculations. The results by this method are in good agreement with other published data and with those independently obtained by the modified residue calculus technique.

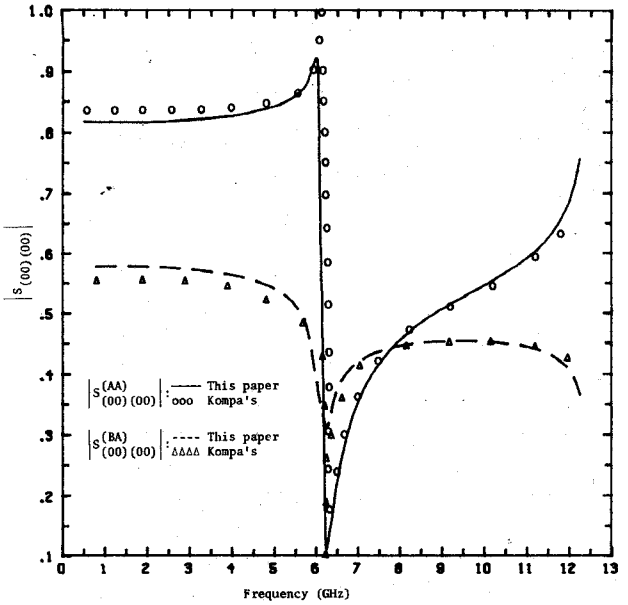

Fig. 9. Comparison with Kompa's results.

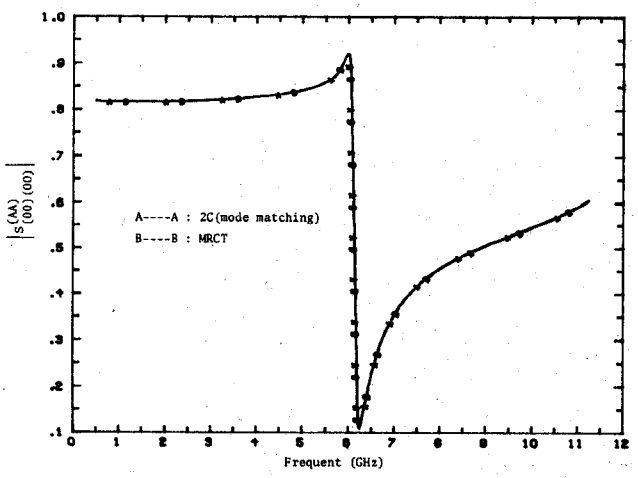

Fig. 10. Comparison with results of modified residue calculus tech nique.

TABLE I
COMPARISON OF THE RESULTS BY MODE-MATCHING METHOD AND BY MRCT*

	Mode Matching	MRCT
$S^{(AA)}_{(00)(00)}$	$0.1837 - j0.02291$	$0.1837 - j0.02297$
$S^{(BA)}_{(00)(00)}$	$-0.7856 + j0.2227$	$-0.7855 + j0.2233$

*Calculations are performed using Kompa's parameters at 2

REFERENCES

[1] I. Wolff, G. Kompa, and R. Mehran, "Calculation method for microstrip discontinuities and *T*-junctions," *Electron. Lett.*, vol. 8, pp. 177–179, Apr. 1972.

[2] G. Kompa, "*S*-matrix computation of microstrip discontinuities with a planar waveguide model," *Arch. Elec. Ubertragung.*, vol. 30, pp. 58–64, 1975.

[3] W. Menzel and I. Wolff, "A method for calculating the frequency-dependent properties of microstrip discontinuities," *IEEE Trans. Microwave Theory Tech.*, vol. MTT-25, pp. 107–112, Feb. 1977.

[4] S. W. Lee, W. R. Jones, and J. J. Campbell, "Convergence of numerical solutions of iris-type discontinuity problems," *IEEE Trans. Microwave Theory Tech.*, vol. MTT-19, pp. 528–536, June 1971.

[5] R. Mittra, T. Itoh, and T. S. Li, "Analytical and numerical studies of the relative convergence phenomenon arising in the solution of an integral equation by the moment method," *IEEE Trans. Microwave Theory Tech.*, vol. MTT-20, pp. 96–104, Feb. 1972.

[6] T. S. Chu and T. Itoh, "Analysis of microstrip step discontinuity by the modified residue calculus technique," submitted to *IEEE Trans. Microwave Theory Tech.*, (Special Issue on Numerical Technique).

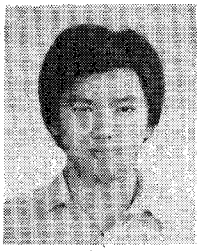

Tak Sum Chu was born in Kowloon, Hong Kong, on October 4, 1960. He received the B.S. degree in electrical engineering from the University of Texas at Austin in 1982. Currently, he is working towards the M.S. degree at the University of Texas.

Tatsuo Itoh (S'69–M'69–SM'74–F'82) received the Ph.D. degree in electrical engineering from the University of Illinois, Urbana, in 1969.

From September 1966 to April 1976, he was with the Electrical Engineering Department, University of Illinois. From April 1976 to August 1977, he was a Senior Research Engineer in the Radio Physics Laboratory, SRI International, Menlo Park, CA. From August 1977 to June 1978, he was an Associate Professor at the University of Kentucky, Lexington, In July 1978, he joined the faculty at the University of Texas at Austin, where he is now a Professor of Electrical and Computer Engineering and Director of the Electrical Engineering Research Laboratory. During the summer 1979, he was a Guest Researcher at AEG-Telefunken, Ulm, West Germany. Since September 1983, he has held the Hayden Head Centennial Professorship of Engineering at the University of Texas. Since September 1984, he has been Associate Chairman for Research and Planning of Electrical and Computer Engineering Department.

Dr. Itoh is a member of the Institute of Electronics and Communication Engineers of Japan, Sigma Xi, and Commission B of USNC/URSI. He serves on the Administrative Committee of IEEE Microwave Theory and Techniques Society and is the Editor of IEEE TRANSACTIONS ON MICROWAVE THEORY AND TECHNIQUES. He is a Professional Engineer registered in the State of Texas.

Yi-Chi Shih (S'80–M'82) was born in Taiwan, the Republic of China, on February 8, 1955. He received the B.Sc. degree from the National Taiwan University, Taiwan, R.O.C., 1976, the M.Sc. degree from the University of Ottawa, Ontario, Canada, in 1980, and the Ph.D. degree from the University of Texas at Austin, in 1982, all in electrical engineering.

In September 1982, he joined the faculty at the Naval Postgraduate School, Monterey, CA, as an Adjunct Professor of Electrical Engineering. Since April 1984, he has been with the Hughes Aircraft Company, Microwave Product Division, Torrance, CA, as a member of the technical staff.